


Pathogenicity and Function Analysis of Two Novel *SLC4A11* Variants in Patients With Congenital Hereditary Endothelial Dystrophy

Tianjiao Zhen¹, Ya Li², Qingge Guo², Shun Yao², Ya You², and Bo Lei ^{1,2}

¹ Henan University People's Hospital, Henan Provincial People's Hospital, Zhengzhou, China

² Henan Branch of National Clinical Research Center for Ocular Diseases, Henan Eye Institute/Henan Eye Hospital, People's Hospital of Zhengzhou University, Henan Provincial People's Hospital, Zhengzhou, China

Correspondence: Bo Lei, Henan Branch of National Clinical Research Center for Ocular Diseases, Henan Eye Institute/Henan Eye Hospital, 7 Weiwu Road, Zhengzhou, Henan 450003, China. e-mail: bolei99@126.com

Received: April 12, 2023

Accepted: August 10, 2023

Published: October 3, 2023

Keywords: *SLC4A11*; congenital hereditary endothelial dystrophy (CHED); compound heterozygous; mitochondria; anti-oxidant

Citation: Zhen T, Li Y, Guo Q, Yao S, You Y, Lei B. Pathogenicity and function analysis of two novel *SLC4A11* variants in patients with congenital hereditary endothelial dystrophy. *Transl Vis Sci Technol.* 2023;12(10):1, <https://doi.org/10.1167/tvst.12.10.1>

Purpose: The purpose of this study was to explore the pathogenicity and function of two novel *SLC4A11* variants associated with congenital hereditary endothelial dystrophy (CHED) and to study the function of a *SLC4A11* (K263R) mutant in vitro.

Methods: Ophthalmic examinations were performed on a 28-year-old male proband with CHED. Whole-exome and Sanger sequencing were applied for mutation screening. Bioinformatics and pathogenicity analysis were performed. HEK293T cells were transfected with the plasmids of empty vector, wild-type *SLC4A11*, and *SLC4A11* (K263R) mutant. The transfected cells were treated with SkQ1. Oxygen consumption, cellular reactive oxygen species (ROS) level, mitochondrial membrane potential, and apoptosis rate were measured.

Results: The proband had poor visual acuity with nystagmus since childhood. Corneal foggy opacity was evident in both eyes. Two novel *SLC4A11* variants were detected. Sanger sequencing showed that the proband's father and sister carried c.1464-1G>T variant, and the proband's mother and sister carried c.788A>G (p.Lys263Arg) variant. Based on the American College of Medical Genetics (ACMG) guidelines, *SLC4A11* c.1464-1G>T was pathogenic, whereas c.788A>G, p.K263R was a variant of undetermined significance. In vitro, *SLC4A11* (K263R) variant increased ROS level and apoptosis rate. Decrease in mitochondrial membrane potential and oxygen consumption rate were remarkable. Furthermore, SkQ1 decreased ROS levels and apoptosis rate but increased mitochondrial membrane potential in the transfected cells.

Conclusions: Two novel heterozygous pathogenic variants of the *SLC4A11* gene were identified in a family with CHED. The missense variant *SLC4A11* (K263R) caused mitochondrial dysfunction and increased apoptosis in mutant transfected cells. In addition, SkQ1 presented a protective effect suggesting the anti-oxidant might be a novel therapeutic drug.

Translational Relevance: This study verified the pathogenicity of 2 novel variants in the *SLC4A11* gene in a CHED family and found an anti-oxidant might be a new drug.

Introduction

Congenital hereditary endothelial dystrophy (CHED; MIM # 217700) is an inheritable disorder of the corneal endothelium that causes bilateral, symmetric, non-inflammatory corneal clouding (edema) at birth or soon after. Patients with CHED present

manifesting as involuntary eye movements (nystagmus) and decreased vision.^{1,2} CHED results in degeneration and dysfunction of endothelial cells of the cornea, and thickening of corneal, which can reach two to three times of the normal thickness. CHED is characterized by thickening of the Descemet's membrane and stromal layers, severe disorganization, and destruction of the stroma structure.^{1,3} Some cases of CHED

may progress to Harboyan syndrome (CDPD, MIM # 217400), which presents manifests as CHED with sensorineural hearing loss.⁴ Corneal transplantation is currently an effective treatment for CHED.

According to the updated International Classification of Corneal Dystrophies in 2015, CHED refers only to the more severe phenotype of autosomal recessive CHED (originally CHED2).⁵ *SLC4A11*, a causative gene of CHED, is located on the short arm of human chromosome 20. The *SLC4A11* gene has 19 exons, of which 19 are coding exons, encoding 891 amino acids.² SLC4A11 protein is widely expressed in the thyroid, trachea, cornea, kidney, salivary gland, and other tissues.⁶ SLC4A11 was identified as a novel electrogenic NH₃⁺/H⁺ co-transporter protein,⁷ which plays an irreplaceable role in the survival, growth, and proliferation of corneal endothelial cells.^{8,9} Ogando et al. found SLC4A11 is localized in the inner mitochondrial membrane and activated SLC4A11 is a mitochondrial uncoupler that can regulate mitochondrial membrane potential (MMP) and reactive oxygen species (ROS) levels.¹⁰ It has been confirmed that SLC4A11 mutant cells are more sensitive to oxidative stress-mediated damage.¹¹ Loss of SLC4A11 activity induces oxidative stress and cells death, leading to CHED, corneal edema, and vision loss.¹⁰ Han et al. constructed an *Slc4a11* knockout mouse model that exhibited characteristic morphological changes of CHED, confirming that deletion of the *SLC4A11* gene could lead to progressive cells damage and apoptosis of corneal endothelial cells.¹² In addition, Liu et al. found that the proliferation of human corneal endothelial cells (HCECs) was inhibited after knocking down *SLC4A11* using short hairpin RNA (shRNA), further confirming that endothelial cells loss was associated with increased cells death caused by activation of apoptotic pathways.¹³ However, the exact mechanism of CHED remains unclear.

So far, 127 mutations in *SLC4A11* gene have been reported, including 90 missense/nonsense mutations, 8 splicing mutations, 4 deletion mutations, 16 small deletion mutations, 2 small insertion mutations, and 7 small insertion and deletion mutations (<https://www.hgmd.cf.ac.uk/ac/gene.php?gene=SLC4A11>). SLC4A11 plays an important role in corneal function. In addition to CHED, mutations in *SLC4A11* also cause Harboyan syndrome (CDPD, MIM # 217400), Fuchs endothelial corneal dystrophy (FECD; MIM # 613267), and may be related to familial keratoconus (KTCN; MIM # 148300).^{14–17} *SLC4A11* mutation-related CHED has rarely been reported in China. In this study, we identified a Chinese family with CHED. Genetic analysis of the target region by high throughput sequencing revealed 2 novel pathogenic variants of

SLC4A11, which expanded the mutation spectrum of *SLC4A11*. We investigated the effect of K263R variant on mitochondrial function and apoptosis in mutated *SLC4A11* gene transfected cells. Furthermore, we tested whether SkQ1, a mitochondria-targeted antioxidant, could protect the mutant gene transfected cells.

Materials and Methods

Clinical Examinations

This study was carried out in accordance with the Declaration of Helsinki and was approved by the Ethics Committee of Henan Eye Hospital. After explaining the risks and benefits of the study to all participants in detail, the participants agreed to participate in this study and signed an informed consent form. The proband, a 28-year-old man, underwent ophthalmic examinations, including best corrected visual acuity (BCVA), slit-lamp microscopy, and swept source optical coherence tomography (SS-OCT; VG200D, SVision Imaging, Luoyang, Henan, China).

Gene Sequencing and Analysis

The peripheral blood of four subjects in the family was extracted and the DNA was extracted using the whole blood DNA extraction kit (DP304; Tiangen, Beijing, China). DNA was sequenced with WES.^{18–20} The captured DNA was eluted, amplified, purified, and sequenced with high-throughput sequencing (NovaSeq 6000, Illumina, San Diego, CA, USA). Sequencing data was analyzed with XYGeneRanger2.0 software (Shanghai Xunyun Biotechnology Co., Ltd., Shanghai, China), TGex software (LifeMap Sciences, Alameda, CA, USA), and EGIS (SierraVast Bio-Medical Technology Co., Ltd., Shanghai, China) software and human genome build hg19 was used as the reference genome. The average sequencing depth was 100X. The variant loci were filtered by ExAC (<http://exac.broadinstitute.org>), gnomAD (<http://gnomad.broadinstitute.org/>), and 1000 Genomes (<https://www.ncbi.nlm.nih.gov/variation/tools/1000genomes/>) public database. Low quality variants and variants with minor allele frequency (MAF) >2% were excluded. Variations identified by WES were validated by Sanger sequencing.^{18–20}

In Silico Analysis and Bioinformatics Analysis

The pathogenicity of genetic variants was evaluated according to the Standards and Guidelines for

the Interpretation of Sequence Variants issued by American College of Medical Genetics (ACMG) in 2015. The pathogenicity of variant sites was predicted by Mutation Taster (<http://www.mutationtaster.org>), CADD (<https://cadd.gs.washington.edu/>), Polyphen2 (<http://genetics.bwh.harvard.edu/pph2/index.shtml>), REVEL (<https://sites.google.com/site/revelgenomics/>), and SIFT software (<https://sift.jcvi.org/>).^{18–20} Protein sequences between different species were compared with Clustal Omega (<https://www.ebi.ac.uk/Tools/msa/clustalo/>). The conserved nature of the variants was analyzed with GERP++ (<http://mendel.stanford.edu/SidowLab/downloads/gerp/index.HTML>) and Weblogo (<http://weblogo.berkeley.edu/logo.cgi>). Three-dimensional structure of protein was built with PyMOL. Mutation effect on the protein structure was predicted online with HOPE (<https://www3.cmbi.umcn.nl/hope/>)²¹ and ExPASy (<http://web.expasy.org/protparam/>).^{18–20}

Plasmid Synthesis

The CDS sequences of *SLC4A11* (NM_032034.4) wild type and c.788A>G, p.K263R were synthesized by Sangon Biotech (Shanghai, China) and cloned into the pcDNA3.1 vector. All sequences of the vector were verified with Sanger sequencing (Sangon Biotech, Shanghai, China).^{18–20}

Cell Culture and Transfection

HEK293T cell line was purchased from the American Type Culture Collection (ATCC, Manassas, VA, USA). Cells were cultured in high glucose DMEM medium containing 10% fetal bovine serum (35-081-CV; Corning, NY, USA) and 100 U per mL of penicillin/streptomycin (32105; Mengbio, Chongqing, China), and placed in a 37°C incubator (5% CO₂).^{18,19} Mycoplasma contamination in HEK293T cells was excluded by the kit (AC16L061; Shanghai Life-iLab Biotech, Shanghai, China).²⁰ Transfection of HEK293T cells was performed with EZ Trans Cell Transfection Reagent (AC04L092; Shanghai Life-iLab Biotech, Shanghai, China) and DNA was conducted in a 3:1 ratio according to the manufacturer's instructions.

Western Blotting

HEK293T cells were seeded into 6-well plates and cultured them in complete DMEM medium for 24 hours after transfection with the plasmids. In RIPA lysis buffer (PC101; Epizyme Biomedical Technology, Shanghai, China) containing a 1X general protease inhibitor (GRF101; Epizyme Biomedical

Technology, Shanghai, China), the HEK293T cells were lysed. To achieve complete lysis, the lysates were further treated with a sonicator (ZQ-650Y; Shanghai Zhengqiao Scientific Instruments, Shanghai, China). After centrifugation at 12,000 rpm for 30 minutes, supernatants were collected and BCA Protein Assay Kit (P0011; Beyotime, Shanghai, China) was used to determine protein concentrations. After mixing with the 5X loading buffer solution, samples were boiled for 5 minutes at 95°C. We resolved protein samples on 7.5% SDS-PAGE gels and transferred them to a PVDF membrane. A PVDF membrane was blocked with 5% skimmed milk powder at room temperature for 2 hours, then incubated overnight at 4°C with specific primary antibodies: SLC4A11 (ER62838, HUABIO, Hangzhou, China) and β -actin (200068-8F10, ZENBIO, Chengdu, China). A PVDF membrane was washed 3 times with TBST, then incubated with secondary antibodies at room temperature for 2 hours. Finally, a PVDF membrane was exposed to enhanced chemiluminescence using a chemiluminescence apparatus (GelView6000Plus, Guangzhou Biolight Biotechnology, Guangzhou, China).^{20,22}

ROS Measurement

Detection of intracellular reactive oxygen levels was conducted by detecting changes in fluorescence intensity of the fluorescent dye DCFH-DA (2,7-dichlorodihydrofluorescein diacetate, S0033; Beyotime, Shanghai, China). According to the manufacturer's instructions, the detection working solution was obtained by diluting DCFH-DA with a serum-free basal medium at a ratio of 1:1000 to a final concentration of 10 μ M. HEK293T cells were seeded into 12-well plates and cultured them in complete DMEM medium for 48 hours after transfection with the plasmids. The cells were washed twice with serum-free basal medium and added to the detection working solution. Then, the cells were placed in the plates in a cell culture incubator set at 37°C and incubated for 30 minutes in the dark. After washing three times with serum-free basal medium, the cells were quickly observed with a fluorescence microscope (Ex/Em = 488/525 nm). Image fluorescence intensity was analyzed using ImageJ software (version 1.52a; National Institutes of Health [NIH]).^{22,23}

Detection of Mitochondrial Membrane Potential

The mitochondrial membrane potential assay was performed using the JC-1 assay kit (C2006; Beyotime,

Shanghai, China).^{22,23} Briefly, HEK293T cells were seeded into 12-well plates, and cultured them in complete DMEM medium for 48 hours after transfection with the plasmids. The cells were digested with EDTA-free trypsin, collected in centrifuge tubes, centrifuged, and incubated for 20 minutes at 37°C in a cell incubator protected from light. The cells were washed twice with JC-1 staining buffer (1X) and detected by flow cytometry for mitochondrial membrane potential, which were expressed as the ratio of JC-1 aggregates to monomer.^{22,23}

Detection of Apoptosis

Apoptosis was detected using the PE Annexin V Apoptosis Assay Kit I (559763; BD Biosciences, Franklin Lakes, NJ, USA). The 10X binding buffer was diluted to 1X with pure water. HEK293T cells were seeded in 12-well plates, and cultured them in complete DMEM medium for 48 hours after transfection with the plasmids. The cells were digested by adding EDTA-free trypsin and collected into centrifuge tubes. The cells were washed twice with cold PBS and resuspended with 100 μ L 1X binding buffer. The solution was added with 5 μ L PE-annexin V and 5 μ L 7-AA, and gently mixed. The cells were incubated at room temperature for 15 minutes and protected from light. Then, 400 μ L 1X binding buffer diluent was added and the apoptosis rate was detected by flow cytometry.²²

Determination of Oxygen Consumption Rate

Oxygen consumption rate of cells, which reflects the function of the respiratory chain, was measured by an XFe analyzer (XFe96; Agilent Seahorse Technologies, Palo Alto, CA, USA).²² HEK293T cells were inoculated at a density of 10,000 cells per well in XF 96-well plates (102601-100; Agilent Seahorse Technologies, Palo Alto, CA, USA) and incubated overnight after 1 hour of standing. Pyruvate (1 mM), glutamine (2 mM), and glucose (10 mM) were added to XF basal medium (103334-100; Agilent Seahorse Technologies), mixed well, and placed at 37°C for preheating. Then the XF96-well plates were moved to an incubator at 37°C without CO₂ for 60 minutes. The XF Cell Mito Stress Kit (103015-100; Agilent Seahorse Technologies) was used to test the respiratory function and mitochondrial metabolism of cells. The diluted reagents Oligomycin (15 μ M), FCCP (5 μ M), and Rotenone/antimycin A (5 μ M) were injected into the probe plate and placed in the Seahorse XFe analyzer for testing. Finally, the protein concentration of each well was measured and

normalized. The results were analyzed using Wave 2.6.3 software.²²

Statistical Analysis

Data were collected from 3 independent experiments, and analyzed by 1-way ANOVA followed by Bonferroni correction, with GraphPad Prism version 7.0 software (GraphPad, La Jolla, CA, USA). Any *P* value < 0.05 was considered statistically significant. All quantitative data were displayed as mean \pm standard deviation (SD).

Results

Clinical Features

The proband (II-1), a 28-year-old man, presented with binocular poor vision and nystagmus since childhood. The BCVA was 0.05 for the left eye and 0.1 for the right eye. Slit-lamp microscopy showed that the corneas of both eyes were foggy and edematous. The depth of the anterior chamber was moderate, the pupil was round with the diameter at 3 mm. The structure of the rest of the eye could not be seen clearly. In the left eye, several vesicles were seen in the central cornea, and corneal leucoma was seen in the inferior temporal region (Fig. 1B). SS-OCT showed that the signal of the corneal stroma of the right eye was uneven. A low-reflection cavity was visible under the corneal epithelium of the left eye, with enhanced light reflection of the posterior corneal tissue (white arrow, Fig. 1C). Neither the father (I-1) nor the mother (I-2) of the proband had ocular signs, although the younger sister (II-2) of the proband had similar clinical manifestations.

Genetic Test Results

After sequencing, 2 new heterozygous variants of *SLC4A11* gene were detected, as shown in Figure 2A. The variant *SLC4A11* c.1464-1G>T was a new splicing mutation located in chr20-3210907. It was not listed in gnomAD_exome (EAS), ExAC (EAS), 1000 Genomes, and other databases. Mutation Taster and CADD predicted that it was harmful. We used spliceAI software (<https://spliceailookup.broadinstitute.org/>) to predict the damage of the splice mutation, and the results showed that it caused Acceptor_loss and the prediction score was 0.99, indicating that the splice mutation was harmful. As a membrane transporter, SLC4A11 protein may mediate signal transduction in the form of receptor. Mutation may lead to

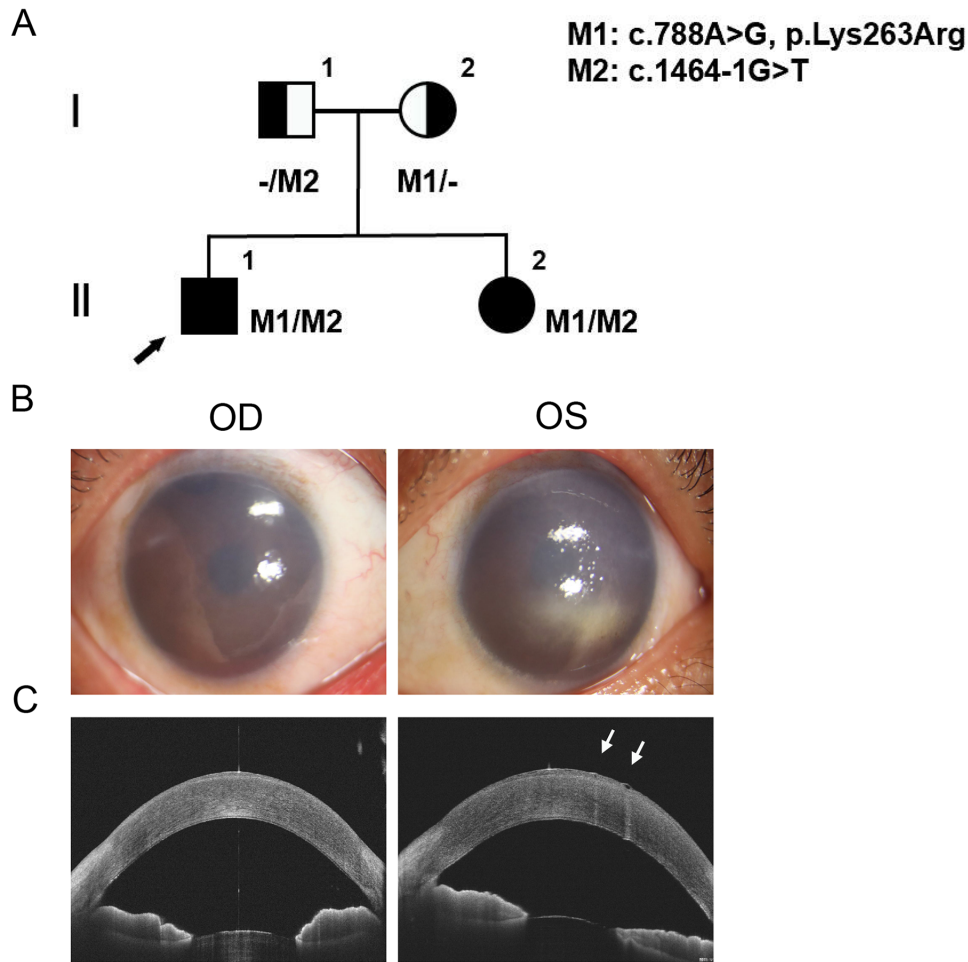


Figure 1. Pedigree and clinical examinations of the proband with congenital hereditary endothelial dystrophy (CHED). **(A)** Pedigree of the proband, indicating by an *arrow*. **(B)** Slit lamp microscopy photograph of the proband. **(C)** Swept source optical coherence tomography (SS-OCT) image of the corneas.

loss or weakening of receptor function, thus affecting mitochondrial function and transport function. According to the ACMG guidelines, the variant was pathogenic: PVS1 + PM2_Supporting.

The variant *SLC4A11* c.788A>G, p.K263R was a novel variant, which was not reported in gnomAD_exome (EAS), ExAC (EAS), 1000 Genomes, and other databases. Mutation Taster, CADD predicted that it was deleterious, and Polyphen2 predicted that it was probably damaging. However, SIFT predicted it was benign. GERP++ showed that the amino acids it encodes were highly conserved. We compared the protein sequences between different species with Clustal Omega (Fig. 2B) and analyzed them by Weblogo (Fig. 2C). The variant site was highly conserved. According to the ACMG guidelines, the variant was a variant of undetermined significance: PM3 + PM2_Supporting + PP3.

The segregation verification showed that the father (I-1) and the sister (II-2) carried the *SLC4A11* c.1464-1G>T variant. The mother (I-2) and sister (II-1) carried the *SLC4A11* c.788A>G, p.K263R variant.

Protein Structure and Function Prediction of K263R

We used HOPE (<https://www3.cmbi.umcn.nl/hope/>) and ExPasy software (<https://www.expasy.org/>) to predict the protein structure, and used PyMOL to make 3D structural models of SLC4A11 (K263R) protein (Fig. 3B). Figure 3A was the schematic structures of the original and the mutant amino acid. The backbone, which was the same for each amino acid, was colored red. The side chain, unique for each amino acid, was colored black. The mutant residue was bigger than the wild-type residue after lysine changed to arginine at position 263. The wild-type

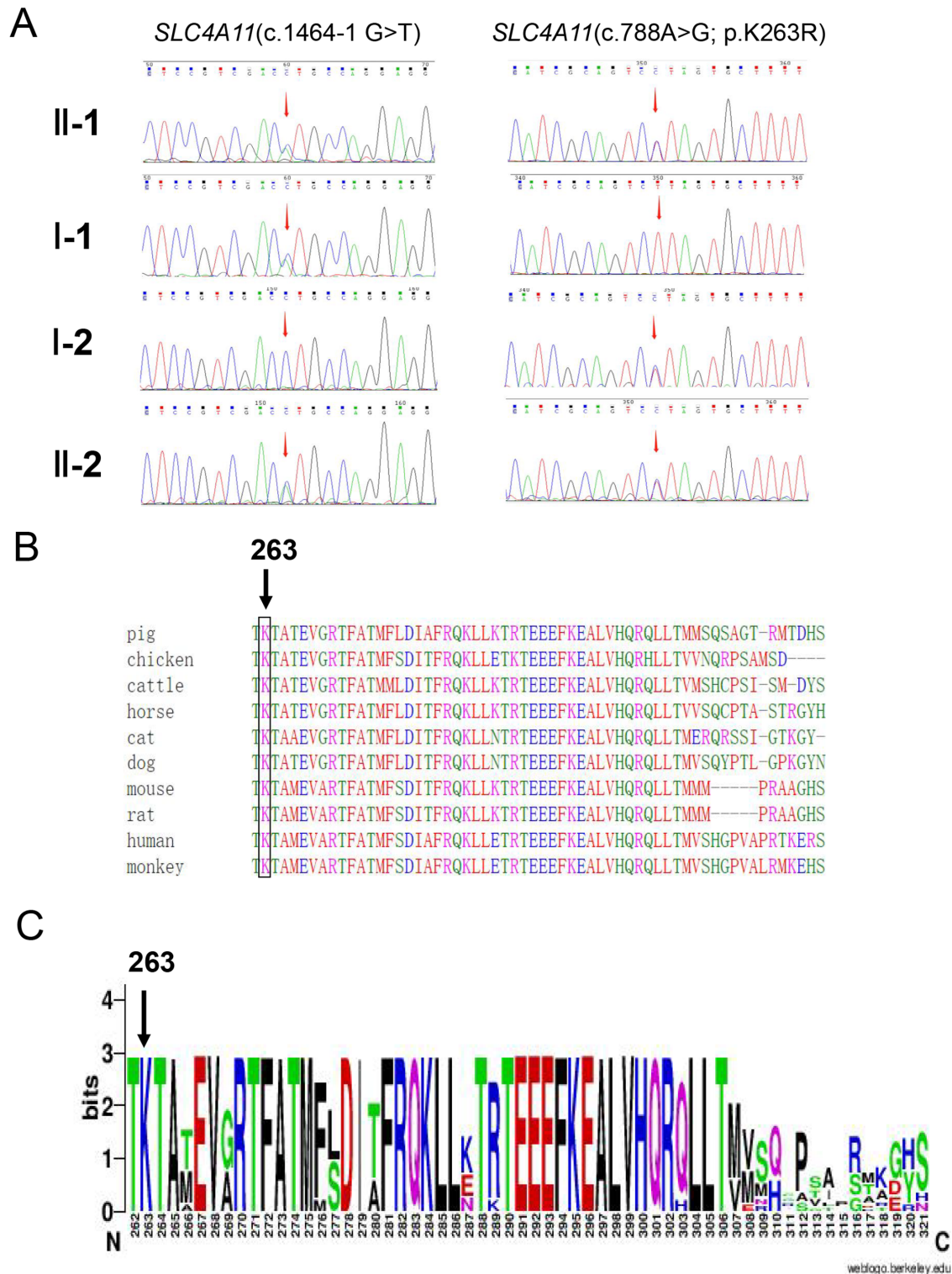


Figure 2. Two novel *SLC4A11* variants (c.1464-1G>T and c.788A>G, p.K263R) were identified in the CHED family. **(A)** Confirmatory Sanger sequencing. **(B)** Clustal Omega software for multiple sequence alignment of p. Lys263 loci among different species. **(C)** The conservativeness of the p. Lys263 locus was analyzed using Weblogo. The horizontal coordinate represents the position of the amino acid and the vertical coordinate represents the conservativeness of the amino acid. The higher the length, the stronger the conservativeness.

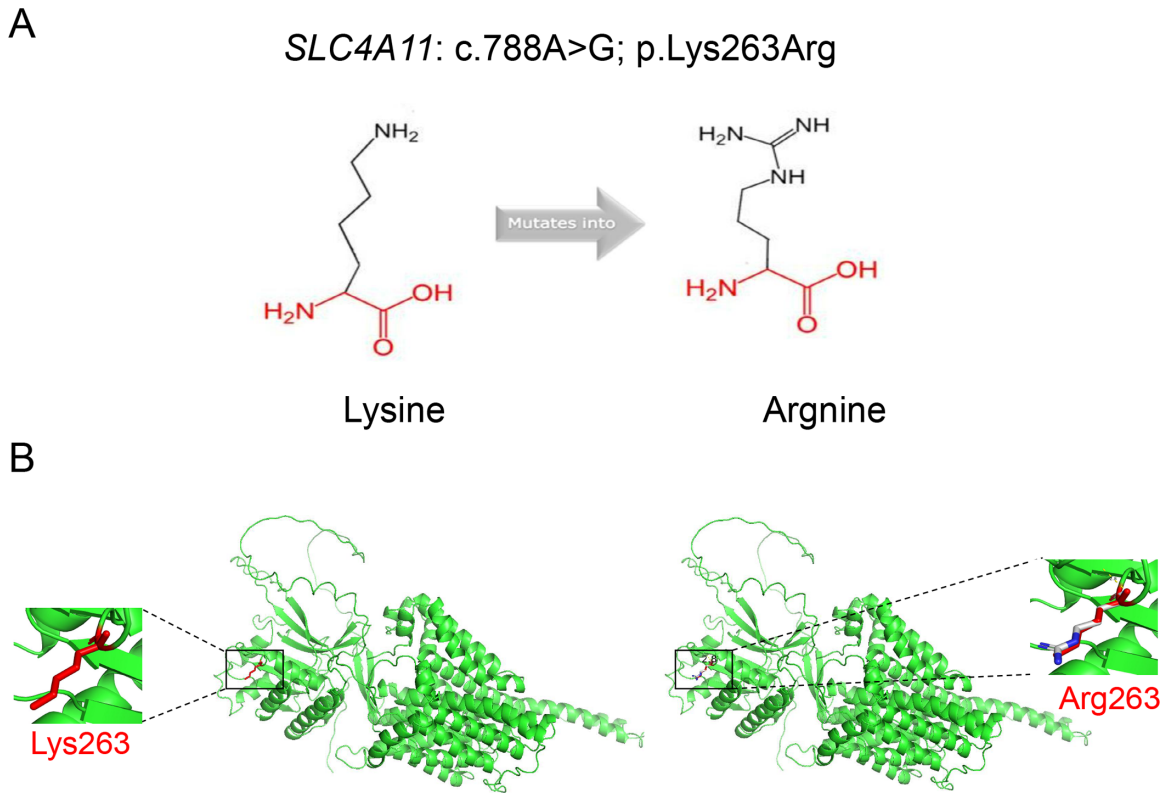


Figure 3. Tertiary structure prediction of wild type and mutant proteins. **(A)** A schematic diagram of the structure of the original amino acid (left) and the mutant amino acid (right). **(B)** Three-dimensional (3D) protein structure comparison by SLC4A11 wild type (left) with c.788A>G, p.K263R (right).

residue was predicted to be located in an α -helix, whereas the mutation caused the replacement of the wild-type residue with another residue that does not prefer α -helices as a secondary structure. Mutant was less stable than wild type.

SLC4A11 Protein Expression Levels

In order to explore the expression levels of SLC4A11 protein, the cDNA plasmids of the wild-type *SLC4A11* and variant *SLC4A11* (K263R) were sub-cloned into pcDNA3.1 (+) expression vectors to HEK293T cells and cultured for 24 hours for Western blotting assay. The results showed that higher SLC4A11 protein expression was seen in the wild type group and the K263R group after plasmid transfection.

K263R Mutation Caused Mitochondrial Dysfunction

In order to investigate whether K263R affected mitochondrial function, the cDNA plasmids of wild-type SLC4A11 and variant SLC4A11 (K263R) were

sub-cloned into pcDNA3.1 (+) expression vectors to HEK293T cells. After 48 hours of incubation, we used the Seahorse XFe analyzer to measure the oxygen consumption rate (OCR), maximum OCR value, and ATP production value of the cells. The results showed that the basal OCR, maximum OCR, and ATP production values of the K263R cells were significantly lower than the empty vector cells and the wild type cells (Fig. 4B).

In order to further verify the mitochondrial function, we detected intracellular ROS and mitochondrial membrane potential. The DCFH-DA fluorescent probe was used to evaluate intracellular ROS levels. Fluorescent images showed that the ROS-positive cells in the K263R group were significantly more than those in the empty vector group and the wild type group (Fig. 5A), indicating that the K263R cells were in a state of higher oxidative stress.

Mitochondrial membrane potential is an important indicator of mitochondrial function. The results of JC-1 assay showed that the K263R group showed higher green fluorescence intensity, but the red fluorescence intensity was much weaker than that of the empty vector and the wild type groups (Fig. 5B), indicating that the mitochondrial membrane potential decreased

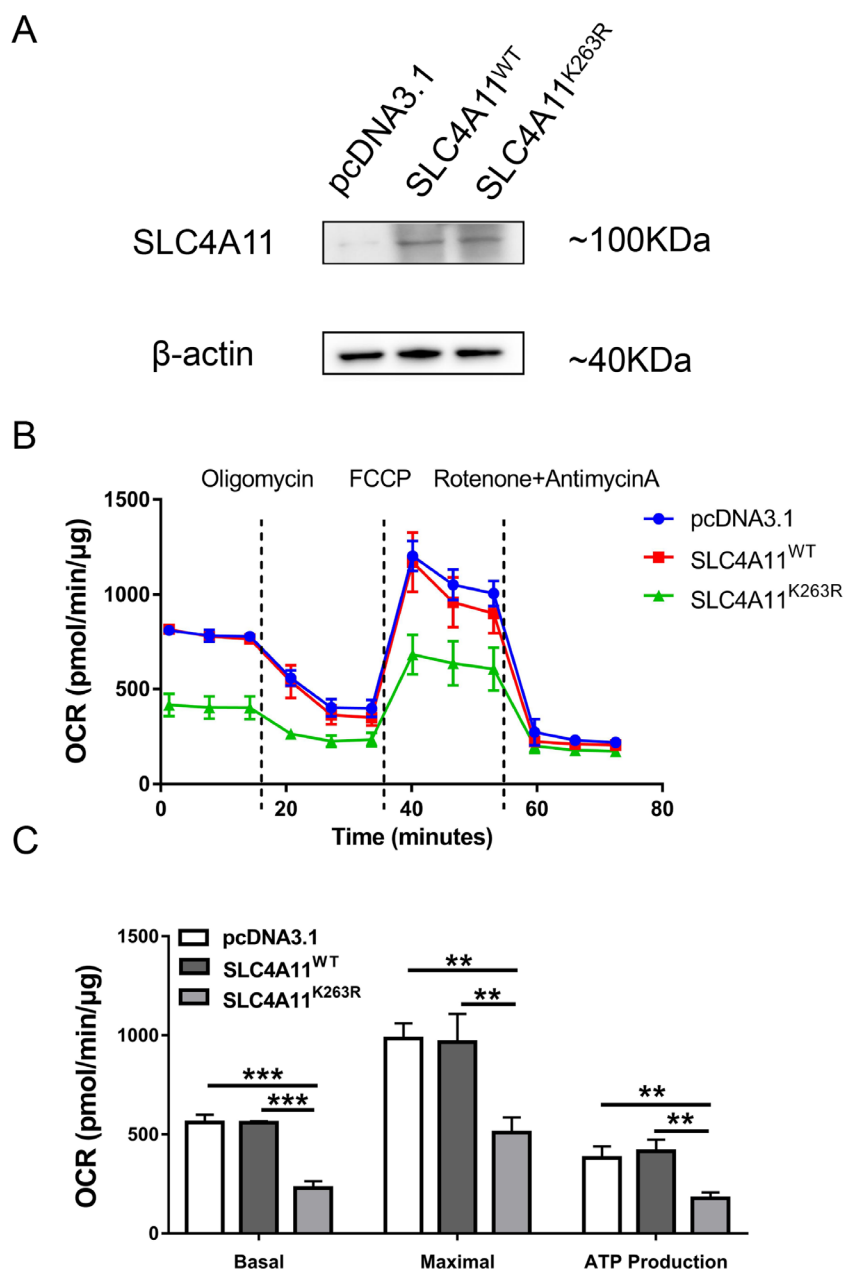


Figure 4. K263R caused dysfunction of the mitochondrial respiratory system. **(A)** The protein expression levels of SLC4A11 were detected using Western blotting. **(B)** Cell oxygen consumption rate measured by XFe analyzer. **(C)** Bar charts show basal respiratory capacity, maximum respiratory capacity and ATP production (values are expressed as mean \pm SD, * $P < 0.05$, ** $P < 0.01$, *** $P < 0.001$, $n = 3$).

significantly. The results further proved that K263R caused mitochondrial dysfunction.

K263R Mutation Promoted Apoptosis

To explore whether the K263R affected cell fate, cell apoptosis was detected 48 hours after plasmid transfection by flow cytometry. The results showed that compared with the empty vector cells and the wild-type cells, the apoptosis rate (Q2 + Q4) of the K263R cells was significantly increased (Fig. 5C).

SkQ1 Improved Mitochondrial Function and Inhibited Apoptosis

Transfected HEK293T cells were treated with SkQ1 (50 nM, HY-100474; MedChemExpress, Monmouth Junction, NJ, USA) for 6 hours, and then incubated for another 48 hours. We tested the ROS level, mitochondrial membrane potential, and cell apoptosis rate. The results showed that SkQ1 treatment significantly decreased the ROS level and cell apoptosis rate but significantly increased the mitochondrial

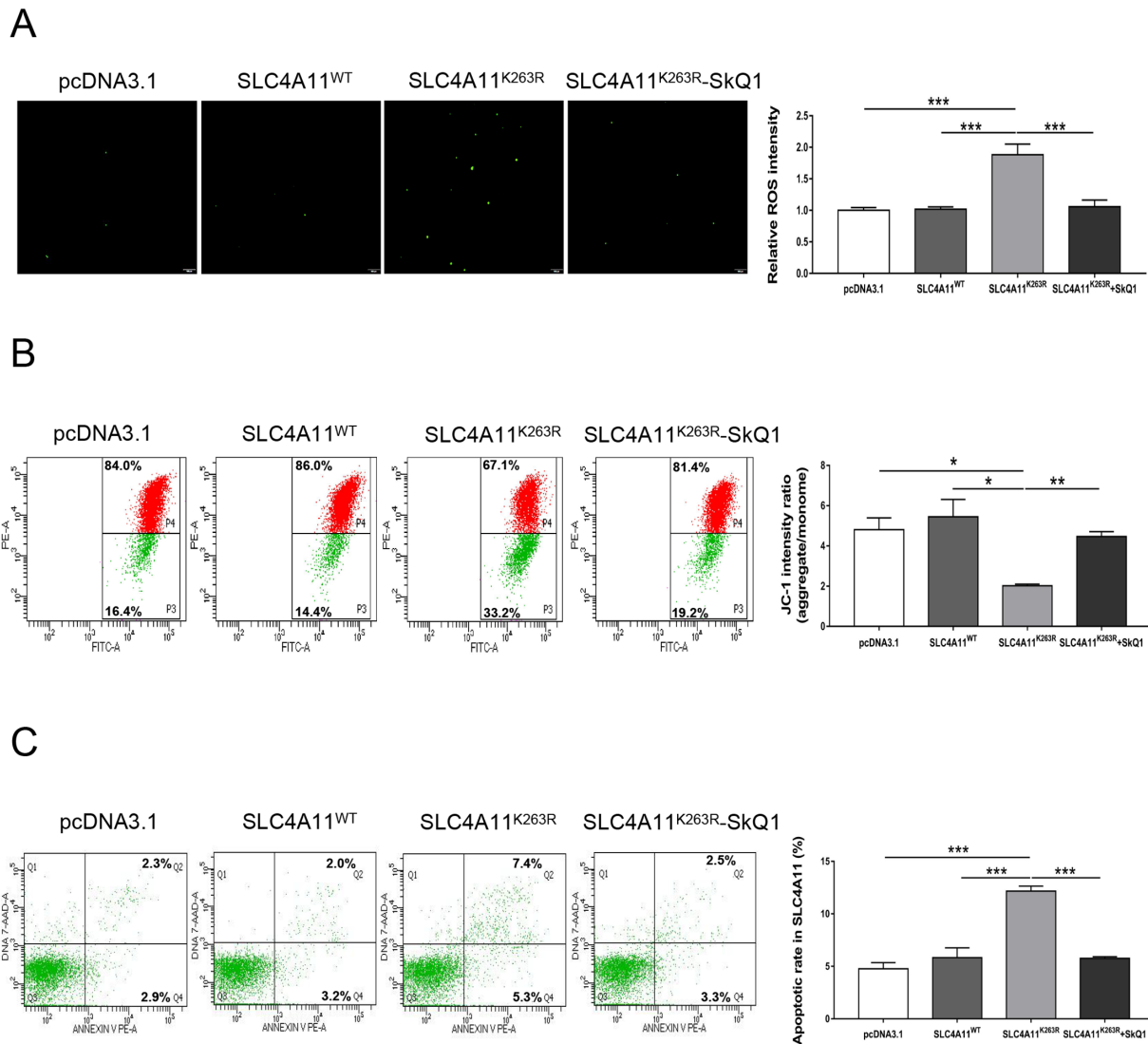


Figure 5. K263R caused impairment of mitochondrial function and apoptosis. **(A)** Detection of mitochondrial membrane potential by using JC-1 staining. The JC-1 aggregates produce red fluorescence, and the JC-1 monomer produces green fluorescence. The ratio of JC-1 aggregates to monomer is used to represent the mitochondrial membrane potential. **(B)** ROS levels were measured in HEK293T cells. **(C)** Flow cytometry was used to quantitatively detect cell apoptosis. Q2 represented late apoptotic cells, and Q4 represented early apoptotic cells. The value of Q2 + Q4 represented the degree of apoptosis (values are expressed as mean \pm SD, * P < 0.05, ** P < 0.01, *** P < 0.001, n = 3).

membrane potential in the K263R cells (Figs. 5A-C). The data suggested that SkQ1 might reverse the oxidative stress-related cell damage caused by K263R variation.

Discussion

The cornea is a transparent membrane located in the anterior wall of the eyeball. It is divided into five layers from the front to the back: epithelium, Bowman's membrane, stroma, Descemet's membrane,

and endothelium.²⁴ The mitochondria, as the powerhouses for cells, are responsible for energy production in the form of ATP.²⁵ Mitochondrial density in corneal endothelium is very high, just below that of photoreceptors in humans, to ensure the production of the high amounts of ATP required to sustain Na⁺/K⁺-ATPase pump function.²⁶ The electron transport chain and oxidative phosphorylation (oxphos) system in the mitochondria are the principal sources of endogenous oxidative stress.²⁷ Oxidative stress describing an imbalance between ROS production and scavenging in cells plays an important role in the degeneration and apoptosis of human corneal endothelial cells.

Many corneal dystrophies, such as CHED and FECD, are associated with oxidative stress.²⁸ CHED mainly manifests as corneal endothelial hypoplasia or corneal endothelial cells degeneration and hypofunction. The clinical features are diffuse corneal edema and opacity in both eyes. Different degrees of visual impairment occur early in life, seriously affecting the visual development of patients, resulting in nystagmus or amblyopia. In this study, the proband had poor visual acuity with nystagmus since childhood. Corneal foggy opacity in both eyes and several vesicle-like bulges in the center of the cornea of the left eye was evident (Fig. 1B). SS-OCT results showed that the light reflection signal of the corneal stroma of the right eye was uneven, and a low-reflection cavity was visible under the corneal epithelium of the left eye, with enhanced light reflection of the posterior corneal tissue (Fig. 1C).

SLC4A11 is a dimer present in the plasma membrane, consisting of an NH₂-terminal 374 amino acids cytoplasmic domain and a 517 amino acids integral membrane domain. The membrane domain of the SLC4A11 protein contains a total of 14 transmembrane regions.^{11,29} SLC4A11 belongs to the SLC4 bicarbonate transporter family,³⁰ however, SLC4A11 does not have bicarbonate transportation activity.^{31,32} SLC4A11 was identified as a novel electrogenic NH₃⁺/H⁺ co-transporter protein⁷ and is basolateral in corneal endothelial cells.³³ Mutations in *SLC4A11* can cause congenital hereditary endothelial dystrophy, Harboyan syndrome, Fuchs endothelial corneal dystrophy, and other diseases.^{14,15,17} Loss of function of SLC4A11 is considered to be an important factor in the death of corneal endothelial cells.¹³

In this study, two novel heterozygous mutations *SLC4A11* c.1464-1G>T and *SLC4A11* c.788A>G, p.K263R were detected. *SLC4A11* c.1464-1G>T was a splicing mutation, which was predicted to be harmful. *SLC4A11* c.788A>G, p.K263R is a novel missense mutation. According to the ACMG guidelines, the variant was of undetermined significance. Therefore, we focused on exploring whether the *SLC4A11* c.788A>G, p.K263R is a pathogenic variant. HEK293 cells hold all human post-translational modifications and they are capable of producing proteins that are similar to those naturally synthesized in humans.³⁴ Therefore, we used HEK293T cells to determine the pathogenicity of *SLC4A11* c.788A>G, p.K263R and to explore the pathogenic mechanisms.

Under physiological conditions, mitochondria are a significant source of ROS, which are involved in both free radical metabolism and energy metabolism.^{35,36} Low concentration of ROS is necessary for the function of cells, but excessive ROS will produce oxidative stress, leading to cell damage and apoptosis.^{37,38} The

basic characteristics of mitochondrial dysfunction are: the disorder of basic mitochondrial functions, such as bioenergy, antioxidation, and regulation, which usually leads to the decline of electron transportation chain function, the decrease of ATP production, the decrease of mitochondrial membrane potential, the increase of ROS production, and eventually leads to cell death. A growing body of evidence supports a strong link between mitochondrial dysfunction and ocular diseases.³⁹ It was reported mutations in *SLC4A11* affected mitochondrial activity leading to corneal endothelial dysfunction.¹¹ We hypothesized that SLC4A11 (K263R) mutation might also affect the cellular response to oxidative stress and lead to mitochondrial dysfunction. We found that SLC4A11 (K263R) mutant increased ROS production, decreased mitochondrial membrane potential, and decreased cellular oxygen consumption rate, but increased apoptosis rate (Fig. 4B, Figs. 5A-C). Our data suggested that *SLC4A11* c.788A>G, p.K263R was a pathogenic variant. Our study expanded the genetic mutation spectrum of *SLC4A11* and provided a new reference for the molecular diagnosis of CHED. Although HEK293T cells do not fully represent the specific pathogenesis of CHED, they might still be a valuable model for studying this disease.

In reference to the previously reported topology model,¹⁵ we found that amino acids 263 is located in the N-terminal domain. The protein sequence between different species showed the amino acids are conserved, indicating that they may have an important function. Kodaganur et al. reported a pathogenic mutation in p.Thr262Ile, but the exact pathogenic mechanism remains unclear.⁴⁰ Roy et al. investigated the physiological roles of SLC4A11 and 4 mutants associated with CHED2 (S213L, R233C, G418D, and T584K). They found that cells containing mutant *SLC4A11* were more susceptible to oxidative stress and mitochondrial damage, and prone to apoptotic.¹¹ These findings are similar to ours.

SkQ1 is a derivative of plastoquinone, which is not only oxidized by ROS but also subsequently reduced by the charged electron transportation chain in the mitochondria. This feature makes these antioxidants “rechargeable” compared to many other mitochondrial-targeting antioxidants.⁴¹ SkQ1 can selectively accumulate in the inner mitochondrial membrane, it can therefore work at very low concentrations, which means that SkQ1, as a potential drug candidate, can reduce the risk of side effects. It was reported recently that SkQ1 could reduce cell damage caused by excessive ROS, effectively regulate mitochondrial membrane potential, reduce corneal damage, restore corneal function, and reduce

ocular surface inflammation.^{42–44} In addition, SkQ1 presented therapeutic effects on dry eye syndrome, uveitis, and conjunctivitis.^{45–48} Evidence from clinical trials indicated that the safety, tolerability, and efficacy of SkQ1 and suggested it may be a promising treatment for dry eye disease.⁴⁴ We used SkQ1 to protect the mitochondrial dysfunction and apoptosis caused by the *SLC4A11* mutation. The results showed that SkQ1 improved mitochondrial function and decreased the apoptosis rate. Thus, SkQ1 might be used for treating CHED, providing more favorable preclinical data are accumulated.

In conclusion, our results broadened both the genotype and phenotype of *SLC4A11* associated CHED. We identified two novel pathogenic variants (c.1464-1G>T and c.788A>G, p.K263R) of *SLC4A11* in a Chinese family with CHED. We found that the mutant SLC4A11 (K263R) caused mitochondrial dysfunction and exaggerated the apoptosis rate. In addition, SkQ1 could protect mitochondrial dysfunction and apoptosis caused by the *SLC4A11* mutation, suggesting that SkQ1 might be a promising therapy for treating this hereditary corneal disorder.

Acknowledgments

Supported by the National Natural Science Foundation of China grants (82071008 and 82271084), and the National Key R&D Plan (2020YFC2008204).

Author Contributions: T.Z. and B.L. were responsible for the conception and design. Y.L., Q.G., S.Y., and Y.Y. were responsible for the data collection. T.Z. was responsible for the data analysis and interpretation. B.L. was responsible for obtaining the fundings. T.Z. and B.L. shared overall responsibility of the study.

Disclosure: T. Zhen, None; Y. Li, None; Q. Guo, None; S. Yao, None; Y. You, None; B. Lei, None

References

- Weiss JS, Moller HU, Lisch W, et al. The IC3D classification of the corneal dystrophies. *Cornea*. 2008;27(Suppl 2):S1–S83.
- Jiao X, Sultana A, Garg P, et al. Autosomal recessive corneal endothelial dystrophy (CHED2) is associated with mutations in SLC4A11. *J Med Genet*. 2007;44(1):64–68.
- Mccartney AC, Kirkness CM. Comparison between posterior polymorphous dystrophy and congenital hereditary endothelial dystrophy of the cornea. *Eye (Lond)*. 1988;2(Pt 1):63–70.
- Desir J, Abramowicz M. Congenital hereditary endothelial dystrophy with progressive sensorineural deafness (Harboyan syndrome). *Orphanet J Rare Dis*. 2008;3:28.
- Weiss JS, Moller HU, Aldave AJ, et al. IC3D classification of corneal dystrophies—edition 2. *Cornea*. 2015;34(2):117–159.
- Cordat E, Casey JR. Bicarbonate transport in cell physiology and disease. *Biochem J*. 2009;417(2):423–439.
- Zhang W, Ogando DG, Bonanno JA, Obukhov AG. Human SLC4A11 is a novel NH₃/H⁺ cotransporter. *J Biol Chem*. 2015;290(27):16894–16905.
- Bahn CF, Falls HF, Varley GA, Meyer RF, Edlhauser HF, Bourne WM. Classification of corneal endothelial disorders based on neural crest origin. *Ophthalmology*. 1984;91(6):558–563.
- Mehta JS, Hemadevi B, Vithana EN, et al. Absence of phenotype-genotype correlation of patients expressing mutations in the SLC4A11 gene. *Cornea*. 2010;29(3):302–306.
- Ogando DG, Choi M, Shyam R, Li S, Bonanno JA. Ammonia sensitive SLC4A11 mitochondrial uncoupling reduces glutamine induced oxidative stress. *Redox Biol*. 2019;26:101260.
- Roy S, Praneetha DC, Vendra VP. Mutations in the corneal endothelial dystrophy-associated gene SLC4A11 render the cells more vulnerable to oxidative insults. *Cornea*. 2015;34(6):668–674.
- Han SB, Ang HP, Poh R, et al. Mice with a targeted disruption of Slc4a11 model the progressive corneal changes of congenital hereditary endothelial dystrophy. *Invest Ophthalmol Vis Sci*. 2013;54(9):6179–6189.
- Liu J, Seet LF, Koh LW, et al. Depletion of SLC4A11 causes cell death by apoptosis in an immortalized human corneal endothelial cell line. *Invest Ophthalmol Vis Sci*. 2012;53(7):3270–3279.
- Riazuddin SA, Vithana EN, Seet LF, et al. Missense mutations in the sodium borate cotransporter SLC4A11 cause late-onset Fuchs corneal dystrophy. *Hum Mutat*. 2010;31(11):1261–1268.
- Vithana EN, Morgan PE, Ramprasad V, et al. SLC4A11 mutations in Fuchs endothelial corneal dystrophy. *Hum Mol Genet*. 2008;17(5):656–666.
- Nowak DM, Karolak JA, Kubiak J, et al. Substitution at IL1RN and deletion at SLC4A11 segregating with phenotype in familial keratoconus. *Invest Ophthalmol Vis Sci*. 2013;54(3):2207–2215.
- Desir J, Moya G, Reish O, et al. Borate transporter SLC4A11 mutations cause both Harboyan

- syndrome and non-syndromic corneal endothelial dystrophy. *J Med Genet.* 2007;44(5):322–326.
18. Zhang L, Li Y, Qin L, Wu Y, Lei B. Autosomal recessive retinitis pigmentosa associated with three novel REEP6 variants in Chinese population. *Genes (Basel).* 2021;12(4):537.
 19. Fu L, Li Y, Yao S, et al. Autosomal recessive rod-cone dystrophy associated with compound heterozygous variants in ARL3 gene. *Front Cell Dev Biol.* 2021;9:635424.
 20. Yang L, Jin X, Li Y, et al. A novel mutation located in the intermembrane space domain of AFG3L2 causes dominant optic atrophy through decreasing the stability of the encoded protein. *Cell Death Discov.* 2022;8(1):361.
 21. Venselaar H, Te Beek TA, Kuipers RK, Hekkelman ML, Vriend G. Protein structure analysis of mutations causing inheritable diseases. An e-Science approach with life scientist friendly interfaces. *BMC Bioinformatics.* 2010;11:548.
 22. Yao S, Zhou Q, Yang M, et al. Multi-mtDNA variants may be a factor contributing to mitochondrial function variety in the skin-derived fibroblasts of Leber's hereditary optic neuropathy patients. *Front Mol Neurosci.* 2022;15:920221.
 23. Zhou Q, Yao S, Yang M, et al. Superoxide dismutase 2 ameliorates mitochondrial dysfunction in skin fibroblasts of Leber's hereditary optic neuropathy patients. *Front Neurosci.* 2022;16:917348.
 24. Delmonte DW, Kim T. Anatomy and physiology of the cornea. *J Cataract Refract Surg.* 2011;37(3):588–598.
 25. Li H, Rukina D, David FPA, et al. Identifying gene function and module connections by the integration of multispecies expression compendia. *Genome Res.* 2019;29(12):2034–2045.
 26. Li S, Kim E, Bonanno JA. Fluid transport by the cornea endothelium is dependent on buffering lactic acid efflux. *Am J Physiol Cell Physiol.* 2016;311(1):C116–C126.
 27. Miyai T. Fuchs endothelial corneal dystrophy and mitochondria. *Cornea.* 2018;37(Suppl 1):S74–S77.
 28. Wojcik KA, Kaminska A, Blasiak J, Szaflik J, Szaflik JP. Oxidative stress in the pathogenesis of keratoconus and Fuchs endothelial corneal dystrophy. *Int J Mol Sci.* 2013;14(9):19294–19308.
 29. Loganathan SK, Lukowski CM, Casey JR. The cytoplasmic domain is essential for transport function of the integral membrane transport protein SLC4A11. *Am J Physiol Cell Physiol.* 2016;310(2):C161–C174.
 30. Alka K, Casey JR. Bicarbonate transport in health and disease. *IUBMB Life.* 2014;66(9):596–615.
 31. Jalimarada SS, Ogando DG, Vithana EN, Bonanno JA. Ion transport function of SLC4A11 in corneal endothelium. *Invest Ophthalmol Vis Sci.* 2013;54(6):4330–4340.
 32. Ogando DG, Jalimarada SS, Zhang W, Vithana EN, Bonanno JA. SLC4A11 is an EIPA-sensitive Na(+) permeable pHi regulator. *Am J Physiol Cell Physiol.* 2013;305(7):C716–C727.
 33. Damkier HH, Nielsen S, Praetorius J. Molecular expression of SLC4-derived Na+-dependent anion transporters in selected human tissues. *Am J Physiol Regul Integr Comp Physiol.* 2007;293(5):R2136–R2146.
 34. Hu J, Han J, Li H, et al. Human embryonic kidney 293 cells: a vehicle for biopharmaceutical manufacturing, structural biology, and electrophysiology. *Cells Tissues Organs.* 2018;205(1):1–8.
 35. Balaban RS, Nemoto S, Finkel T. Mitochondria, oxidants, and aging. *Cell.* 2005;120(4):483–495.
 36. Kausar S, Wang F, Cui H. The role of mitochondria in reactive oxygen species generation and its implications for neurodegenerative diseases. *Cells.* 2018;7(12):274.
 37. Kryston TB, Georgiev AB, Pissis P, Georgakilas AG. Role of oxidative stress and DNA damage in human carcinogenesis. *Mutat Res.* 2011;711(1–2):193–201.
 38. Valko M, Rhodes CJ, Moncol J, Izakovic M, Mazur M. Free radicals, metals and antioxidants in oxidative stress-induced cancer. *Chem Biol Interact.* 2006;160(1):1–40.
 39. Jarrett SG, Lewin AS, Boulton ME. The importance of mitochondria in age-related and inherited eye disorders. *Ophthalmic Res.* 2010;44(3):179–190.
 40. Kodaganur SG, Kapoor S, Veerappa AM, et al. Mutation analysis of the SLC4A11 gene in Indian families with congenital hereditary endothelial dystrophy 2 and a review of the literature. *Mol Vis.* 2013;19:1694–1706.
 41. Kelso GF, Porteous CM, Coulter CV, et al. Selective targeting of a redox-active ubiquinone to mitochondria within cells: antioxidant and antiapoptotic properties. *J Biol Chem.* 2001;276(7):4588–4596.
 42. Skulachev VP. Cationic antioxidants as a powerful tool against mitochondrial oxidative stress. *Biochem Biophys Res Commun.* 2013;441(2):275–279.
 43. Zinovkin RA, Romaschenko VP, Galkin Ii, et al. Role of mitochondrial reactive oxygen species in age-related inflammatory activation of endothelium. *Aging (Albany NY).* 2014;6(8):661–674.

44. Petrov A, Perekhvatova N, Skulachev M, Stein L, Ousler G. SkQ1 ophthalmic solution for dry eye treatment: results of a phase 2 safety and efficacy clinical study in the environment and during challenge in the controlled adverse environment model. *Adv Ther.* 2016;33(1):96–115.
45. Zinovkin RA, Zamyatnin AA. Mitochondria-targeted drugs. *Curr Mol Pharmacol.* 2019;12(3):202–214.
46. Antonenko YN, Avetisyan AV, Bakeeva LE, et al. Mitochondria-targeted plastoquinone derivatives as tools to interrupt execution of the aging program. 1. Cationic plastoquinone derivatives: synthesis and in vitro studies. *Biochemistry (Moscow).* 2009;73(12):1273–1287.
47. Skulachev VP, Anisimov VN, Antonenko YN, et al. An attempt to prevent senescence: a mitochondrial approach. *Biochim Biophys Acta.* 2009;1787(5):437–461.
48. Iomdina EN, Khoroshilova-Maslova IP, Robustova OV, et al. Mitochondria-targeted antioxidant SkQ1 reverses glaucomatous lesions in rabbits. *Front Biosci (Landmark Ed).* 2015;20(5):892–901.